

# Diamond-VeNOM: a high-speed slope profiler for characterizing X-ray mirrors

Ioana-Theodora Nistea\*, Simon G. Alcock, Murilo Bazan da Silva, K. Sawhney  
Diamond Light Source Ltd, Harwell Science and Innovation Campus, Didcot, OX11 0DE, UK

## ABSTRACT

The Diamond-NOM slope profilometer has been in operation for more than 15 years in the Optics Metrology Lab at Diamond. It is an established instrument for accurate characterisation of X-ray optics for synchrotron and XFEL beamlines. However, continuous improvements in the fabrication quality of X-ray optics now means that polishing errors are comparable in magnitude to instrumental systematic errors. For X-ray optics with slope errors  $\ll 100$  nrad rms and height errors  $< 1$  nm, repeated measurements in multiple configurations are typically required to obtain accurate metrology data. To tackle such issues, we have developed a new instrument: the Diamond-VeNOM (velocity-NOM). VeNOM utilizes multiple autocollimators, synchronized with motion stages, to simultaneously measure the optical surface and monitor parasitic motion errors. A significant increase in measurement speed is achieved using 10x faster Elcomat5000 autocollimators. Motion trajectories are aligned with autocollimator data by temporarily blocking the beam paths using electronic shutters, based on triggering signals from positional encoders. Enhanced motion control capabilities allow user-defined velocity profiles of the scanning stage, coordinated with motorised pitch of the optic under test throughout the scan. This enables innovative dynamic scanning strategies, including on-the-fly, free-form, automated nulling of the optical surface throughout the scan to reduce systematic errors.

**Keywords:** Slope profilometry, Autocollimator, Diamond-NOM, X-ray mirrors

[\\*ioana.nistea@diamond.ac.uk](mailto:ioana.nistea@diamond.ac.uk); [www.diamond.ac.uk](http://www.diamond.ac.uk)

## 1. INTRODUCTION

Since 2007, the Diamond-NOM [1] has played a major role in the Optics Metrology Lab (OML) [2] at Diamond. Metrology feedback has helped to optimally clamp hundreds of X-ray mirrors and diffraction crystals into opto-mechanical holders for beamline operation [3]. With sufficient averaging, the sensitivity of the autocollimator (AC) of the Diamond-NOM can resolve ultra-small angle changes of  $\ll 20$  nrad.

Several NOM profilers now employ two or more AC's to simultaneously measure the mirror under test and the parasitic angular errors of the scanning stage [4,5]. However, despite reducing the path-length dependency issues, this doesn't solve all problems: calibration at a National Metrology Institute (NMI) is only valid for a specific curvature and reflectivity of the test mirror.

To achieve fast and accurate scanning, we have developed the Diamond-VeNOM (velocity-NOM): a high-speed, slope profiler of X-ray optics which utilizes 10X faster, Elcomat5000 autocollimators (from Moller-Wedel) which are synchronized with movement of the multiple motion stages. The VeNOM concept combines the advantages of previous schemes to further minimize systematic errors. It also incorporates two, new distinct features: the scan head is programmed to execute an arbitrary, free-form speed profile during the scan; and the optic under test is simultaneously pitched in coordination. Arbitrary angular profiles can be purposefully chosen to null instrumental systematic errors of the autocollimators and environmental perturbances, thereby improving measurement accuracy.

## 2. EXPERIMENTAL

### 2.1 Instrument geometry

The classical Diamond-NOM uses a single Elcomat3000 electronic autocollimator (Möller-Wedel, Germany) and a high-grade pentaprism, mounted on an X-axis air-bearing stage (Q-Sys, Netherlands), to scan an aperture-defined region of an autocollimator beam along the length of the optic under test. A secondary, orthogonal, air-bearing translation stage (Y-axis) and motorized pitch stage  $R_y$  change the sagittal location and pitch of the mirror relative to the autocollimator

beam. Figure 1 shows the upgraded hardware of the new Diamond-VeNOM system which enables high-speed, synchronized operation of all components. Elcomat autocollimators simultaneously monitor all moving components of the system.

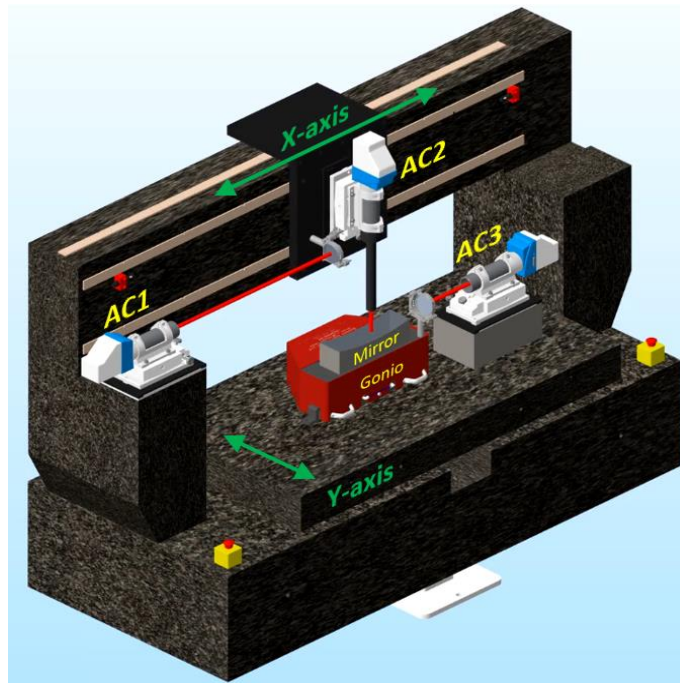


Figure 1. Model of the Diamond-VeNOM, showing the three autocollimators (AC) which simultaneously measure: parasitic angles of the scan carriage during translation along the X-axis (AC1); the surface of the mirror under test (AC2); and the pitch angle of the goniometer (AC3). Autocollimator and motion data are synchronized using new controls hardware described in Section 2.2.

The first autocollimator, AC1, fixed on the left-hand granite column, observes a large aperture ( $> 10\text{mm}$  diameter), flat mirror attached to the X-axis stage to monitor small ( $< 5 \mu\text{rad PV}$ ), parasitic angle errors  $\theta_y$  and  $\theta_z$  (rotations about the Y and Z axes) during translation. Path-length linearity errors of the AC are minimized for small angles [6]. The second autocollimator, AC2, is mounted on the X-axis scanning stage and directly measures a small region ( $\sim 3.5 \text{ mm}$  diameter) of the mirror under test at a nominally fixed distance. Nulling the measured angle using the pitch stage reduces the influence of angle dependent errors of AC2 originating from curvature and / or reflectivity of different optics. The third autocollimator, AC3, attached to the granite Y-stage, observes a large aperture, flat mirror mounted on the pitch stage at a nominally fixed distance. AC3 can be calibrated at an NMI over a wide range of angles for fixed experimental parameters, thereby further reducing systematic error and improving accuracy.

## 2.2 Hardware upgrade and control logic

Dynamic scanning requires coordination and synchronization of multiple components at rates that surpass the capabilities of the classical NOM's instrumentation hardware. Consequently, the following upgrades were made to the hardware and software infrastructure of the Diamond-VeNOM:

- New Elcomat5000 autocollimators with an acquisition rate of 250 Hz, which represents a tenfold increase in speed compared to the older Elcomat3000 model.
- Delta-Tau "Power PMAC" controller for NOM's motion stages (Q-Sys), which offers enhanced precision and higher-speed operation.

- Panda input/output box to facilitate high-speed synchronization and complex management of multiple encoder inputs and outputs triggering signals to coordinate dynamic data acquisition.
- Serial-to-Ethernet terminal server (MOXA box) to streamline data handling from the autocollimators and establish a direct connection with Diamond’s EPICS motion controls network for enhanced data accessibility and synchronization with other system components.
- Mechanical shutters (triggered by the PandaA box) embed null values in the AC data which helps to precisely align angle data relative to motion positioning throughout scanning.

These upgrades collectively ensure that the VeNOM system is well-equipped to meet the demanding requirements of dynamic scanning, including higher-speed and more precise metrology data acquisition. The control logic of the Diamond VeNOM, as illustrated in Figure 2, is orchestrated within the Malcolm environment. Malcolm is a specialized data coordination framework developed at Diamond, which operates above the EPICS channel access layer, and offers advanced configuration capabilities, including the ability to define arbitrary, freeform motion trajectories, including variable speed and acceleration during each scan. Position encoder readback plays a central role in this control logic. It serves primarily to control the dynamic motion of the X-stage, but can also manage the behaviour of other components, such as the pitch stage and opening/closing of the mechanical shutters.

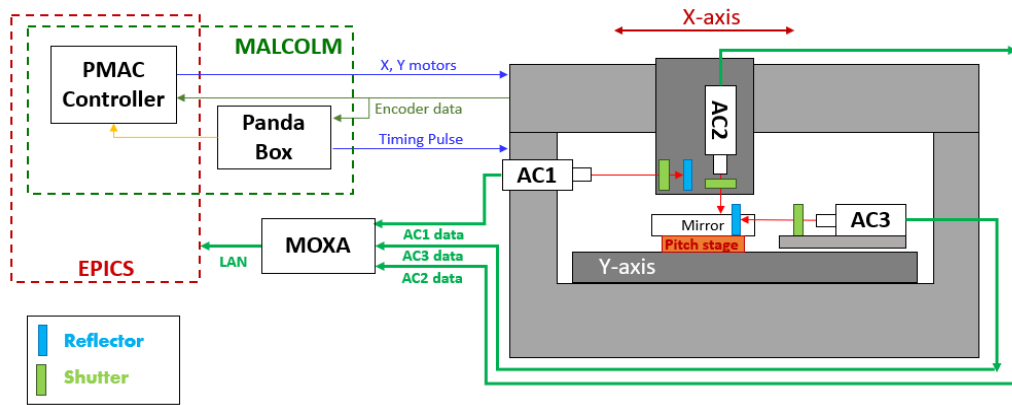


Figure 2. Control logic of the upgraded VeNOM system, showing how the Malcom layer coordinates interactions between the three autocollimators, the triggered shutters, and the motion encoders of the scan axis and pitch stage.

### 2.3 Data synchronization with mechanical shutters

Elcomat autocollimators lack high-speed triggering capabilities. To achieve synchronization between multiple autocollimators and positional encoders, we have incorporated electro-mechanical shutters into the optical path. These shutters are open by default, letting the autocollimator beam pass through. Once triggered by TTL signals from the PandaA box, shutters simultaneously block the optical path of all autocollimators for a brief interval (typically 20 milliseconds). The trigger action is programmed to occur when the X-stage reaches a series of user-defined positions. Shutters introduce null values at specific points within each autocollimator data stream. These null values serve as synchronization markers to align all autocollimator data with readings from the position encoders and measured location on the optical surface. This synchronization process is essential for precise correlation and analysis during dynamic scanning operations.

Figure 3 demonstrates a representative application of synchronization logic. The upper left image (purple lines) shows all shutters are triggered to close (logical value = 1) when the positional encoder readback confirms that the X-stage has reached specific, user-defined locations of X = 10, 30, 50, 70, and 90 mm. In this example, the X-stage is programmed to execute a non-linear velocity profile (constant acceleration), as shown in the black curve in the lower left chart. Note that although the shutter pulses are evenly distributed in space, they are not evenly distributed in time. As seen in the right column of images in Figure 3, null values are incorporated into each of the autocollimator data streams.

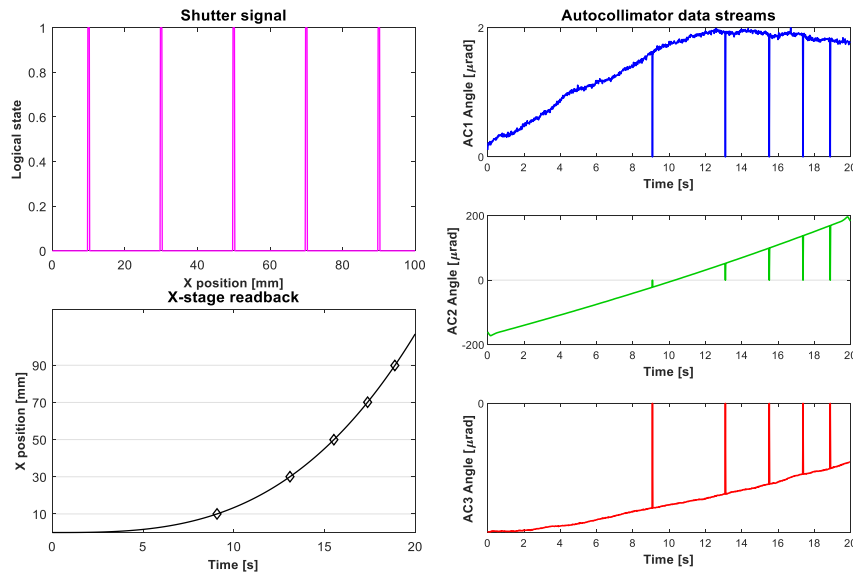


Figure 3. Diagram showing an example of synchronization logic to embed null values into each autocollimator data stream by using shutter pulses triggered to occur when the X-axis scanning stage reaches a series of user-defined locations, including free-form velocity and acceleration profiles.

### 3. RESULTS

#### 3.1 Noise levels of the Elcomat5000 autocollimator

Stability tests were conducted for the new Elcomat5000 autocollimator mounted on a passively damped, pneumatic optical table, situated within a protective enclosure. The autocollimator observed a flat mirror (25 mm diameter) located ~ 200 mm away. A beam-defining iris was placed a few millimeters away from the mirror. As shown in Figure 4, the optical path was optionally shielded to reduce air turbulence and external influences.

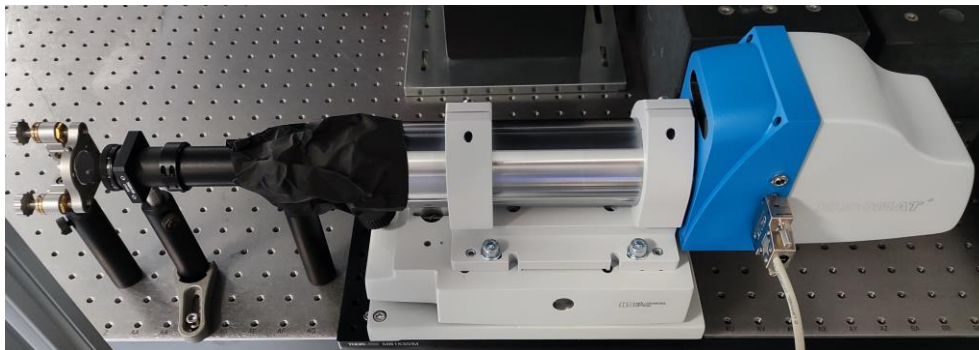


Figure 4. Noise level tests of the new Elcomat5000 autocollimator monitoring a fixed, flat mirror using a variable sized iris.

In Figure 5, the power spectral density (PSD) of the angle measured by the Elcomat5000 is shown for various iris diameters (between 4 and 6 mm), with and without shielding of the air path. For comparison, data from an Elcomat3000 mounted on the Diamond-NOM is included. To improve statistics, the long-duration data stream was batched into smaller temporal blocks. Calculating the average FFT for all blocks (within a specific experimental configuration) reduced random noise to aid visualization of the frequency response of the autocollimators.

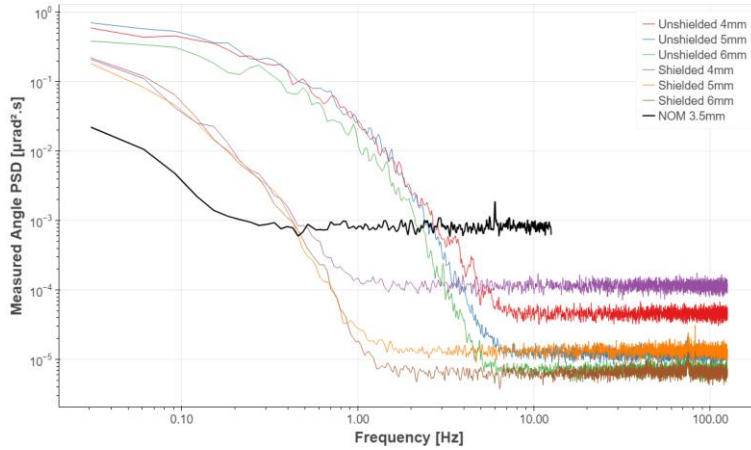


Figure 5. Averaged PSD showing the noise levels of the old Elcomat3000 (thick, black curve) and the new Elcomat5000 autocollimator, with and without path shielding, for different diameters of beam-defining apertures.

As expected, path shielding leads to a significant reduction in the PSD amplitude of autocollimator data for all iris diameters, especially below 8 Hz. For the shielded path, the Elcomat5000 data is less noisy than the Elcomat3000 above  $\sim 0.5$  Hz. Two resonance frequencies were detected in the ‘shielded’ datasets at  $\sim 44.2$ Hz and  $\sim 79.3$ Hz. These are induced by floor vibrations (transmitted via the optical table) and the ventilation system (transmitted via the roof of the thermal enclosure). As seen in Figure 5 and Figure 6, measurement noise is asymptotically reduced towards  $\sim 25$  nrad rms as the aperture diameter was increased. The smallest diameter was in this study was 3 mm, which increased noise levels to  $\sim 70$  nrad rms.

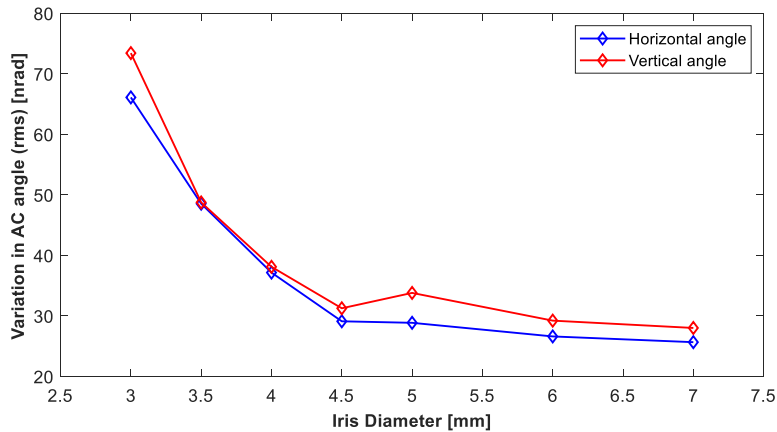


Figure 6. Root-mean-square noise levels of the Elcomat5000 autocollimator as a function of the diameter of a beam defining aperture.

### 3.2 Mechanical shutters

Initial testing of the mechanical shutters consisted of varying the pulse duration of the shutters to block each autocollimator beam. Ideally, the shortest duration signal would be chosen to minimize loss of information about the optical surface. As seen in Figure 7, the shortest pulse signal from the shutter was just over 20 ms, corresponding to 6 readings from the Elcomat5000 (which records angles at 4 ms intervals). However, variation in the duration of the pulse signal could be desirable in a future scenario to uniquely distinguish between specific locations on the optical surface, or to encode experimental parameters into the data. For example, longer pulses to encode the ends of the optical surface, or variations in the pulse width as a function of the pitch angle.

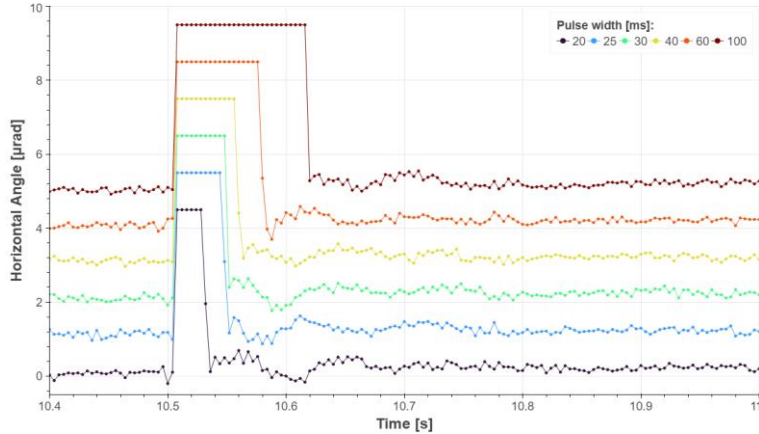


Figure 7. Series of Elcomat5000 acquisitions with a range of demand pulse widths (20, 25, 30, 40, 60, and 100 ms). Scans are aligned on the leading edge of the shutter pulse and offset vertically for clarity.

The shutters provided a reliably method to block each autocollimator beam. However, in certain instances, the action of the mechanical shutters influences other aspects of the experimental apparatus. For example, damped oscillations are observed in Figure 7 in the autocollimator data immediately after the shutter opens. Such oscillations decay within a few tenths of a second, but this still causes loss of data about the optical surface. Mechanical vibrations from the activation of one shutter were also observed to influence the performance of other autocollimators. For example, in Figure 8, when only the shutter for AC2 was triggered, an effect was induced in AC1. This is attributed to the fact that the shutter for AC2 and the reflector for AC1 are both mounted on the X-axis air-bearing stage. Conversely, AC3 is impervious to the shutter activity of AC2, since AC3 and its reflector are mounted on the heavy granite of the Y-axis, which is decoupled from the X-axis.

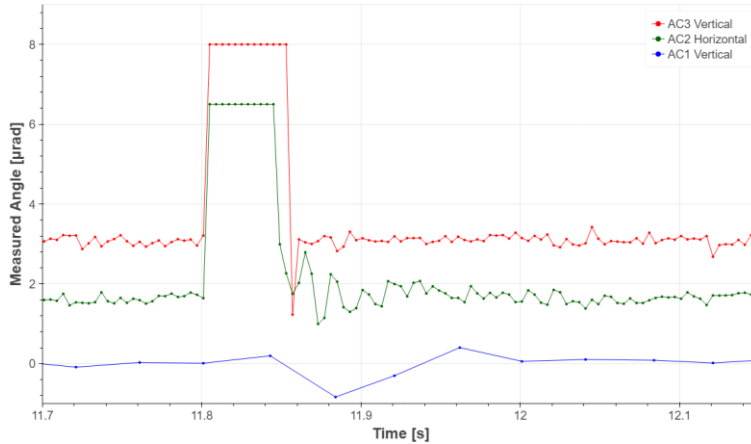


Figure 8. Angular variations observed by each autocollimator after closing only the shutter for AC2. Mechanical vibrations induced in the X-axis stage by the shutter also cause a disturbance to AC1. AC3 is mechanically decoupled from the other two and hence does not observe angle vibrations. Note that the 25 Hz acquisition rate of AC1 (Elcomat3000) does not have sufficient temporal sensitivity to register the ~ 50 Hz ringing effect which is visible in the faster AC2 (Elcomat5000) data.

Time delays from all system components were calibrated by varying the experimental parameters and observing the effects on the autocollimator data. Contributions to the time-lag include: the X-axis encoder readback rate; mechanical shutter latency; and processing time to receive inputs and trigger outputs. A shutter test was performed to compare the pulse delays relative to the target position. Shutter pulses of 100 ms duration were applied to fly-scans with various velocities of the X-axis. Angle data was aligned along the X-direction by comparison with an earlier, step scan of the

same mirror. “Roll-off” slope features, at each end of the optic, were used as alignment fiducials, as seen in Figure 9. Third-order polynomials were removed to aid visualisation. A variable, spatial offset was observed for null values from the target position, which increased with scan velocity. When plotted against time, these spatial delays convert into a temporal delay of 20 – 30 ms between the moment the X-axis passes the target position and the shutter pulse registering in the autocollimator data. Further investigation and optimization of such factors is required to further improve the synchronisation of pulses.

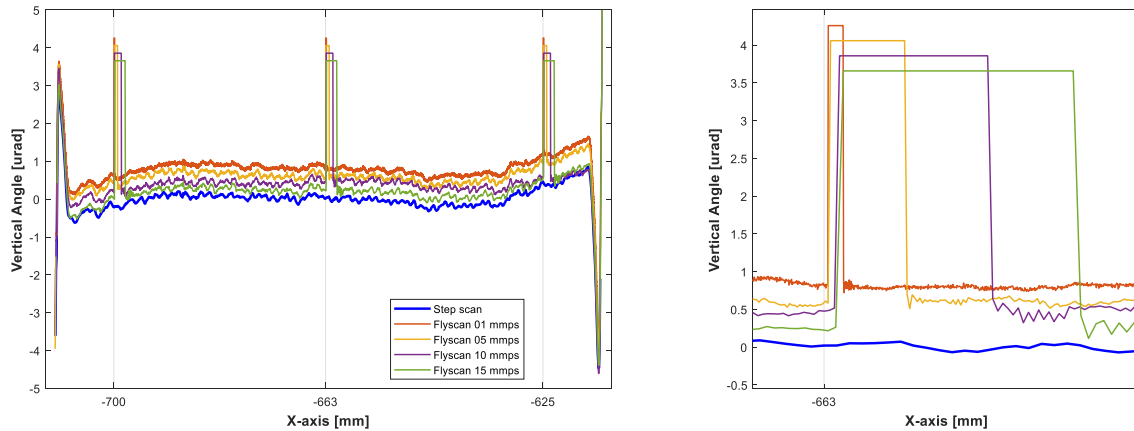


Figure 9. Shutter pulse delay tests, showing: (left) a comparison between AC2 datasets obtained at different scan velocities and the step scan measurement of the optical surface; and (right) a zoomed version on the central shutter pulse ( $X = -663$  mm) to highlight the delays at the various scan velocities relative to the target location.

### 3.3 X-stage parasitic error

Another systematic error to be calibrated in the parasitic angle error of the X-stage. Such errors are well studied for quasi-static step scans, but the motion performance of the X-axis could change for variable speed and accelerations. To investigate, a comprehensive series of tests were performed. The geometry for this investigation is shown in Figure 10. Two autocollimators (Elcomat3000 at AC1, and Elcomat5000 at a modified position for AC3) both monitor the same reflective cube mounted on the X-axis. This setup provides enhanced time / space resolution data for parasitic angle readings, which is particularly useful when monitoring higher speed scans.

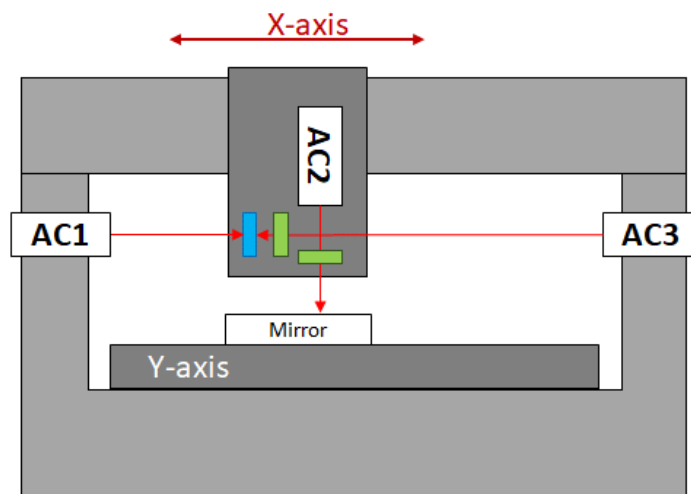


Figure 10. Diagram of the triple AC setup used to investigate parasitic angle errors during scanning of the X-axis translation stage. The main difference relative to the VeNOM geometry is the absence of the pitch stage, and reassignment of AC3 to provide a secondary, higher-speed monitoring of the X-axis.

Figure 11 shows the parasitic angles during translation of the X-axis translation, as measured by AC3, for different types of motion. Each curve is the average of 20 repeated scans. The parasitic angle error of the X-axis has a peak to valley of  $\sim 1.5 \mu\text{rad}$ . The fly-scans at  $20 \text{ mm s}^{-1}$  (maximum speed of the X-stage) have a slight difference in the low frequency component compared to the lower speeds, but there is very good repeatability between all other speeds. The  $1 \text{ mm s}^{-1}$  fly-scan is most comparable with the pseudo-static step-scan. There is also the expected loss of high frequency features for the faster scans.

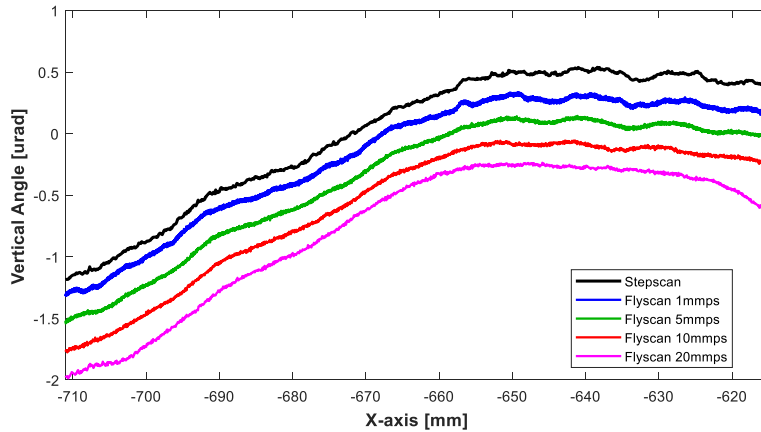


Figure 11. Parasitic pitch angle errors (rotation about Y axis), as measured by an Elcomat5000 at AC3, when the X-stage was scanned at various speeds. For comparison, data is also included for the quasi-static step-scans, which has a wait time of 2 seconds between completion of each motion step and the start of AC acquisition.

To assess whether the Elcomat3000, with its lower acquisition rate, is well-suited for dynamic scanning, a comparison is shown in Figure 12. For a fly-scan speed of  $1 \text{ mm s}^{-1}$  there is excellent agreement, despite the significant difference in acquisition rates. These preliminary results provide confidence about the suitability of the Elcomat3000 for dynamic scanning.

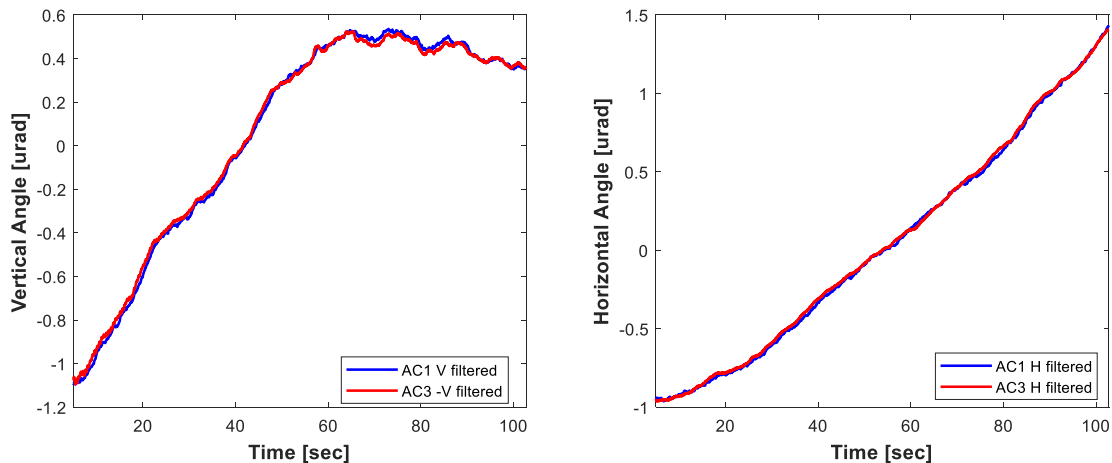


Figure 12. Parasitic angle errors observed by the two models of autocollimator during translation of the X-axis at a constant fly-scan speed of  $1 \text{ mm s}^{-1}$ . Excellent agreement is obtained, providing confidence that the slower Elcomat3000 is still suitable to monitor certain aspects of dynamic scanning.

### 3.4 Motorized pitch stage

The motorized pitch stage in this study is a Kohzu goniometer with a stepper motor operating in open-loop. With AC3 repositioned in the geometry shown in Figure 1, the motion characteristics of the pitch stage were investigated. Angle stability of the pitch stage was assessed after moving to a demand angle. Angular drift of  $\sim 120$  nrad (peak-to-valley) was observed over a period of 50 minutes. The process of returning the pitch stage to a specific angle (always from the same starting point) was repeated multiple times, and good repeatability was achieved. The average of such scans is shown in Figure 13. This demonstrates the necessity to continuously monitor angular drifts of the pitch stage, even for constant demand angles.

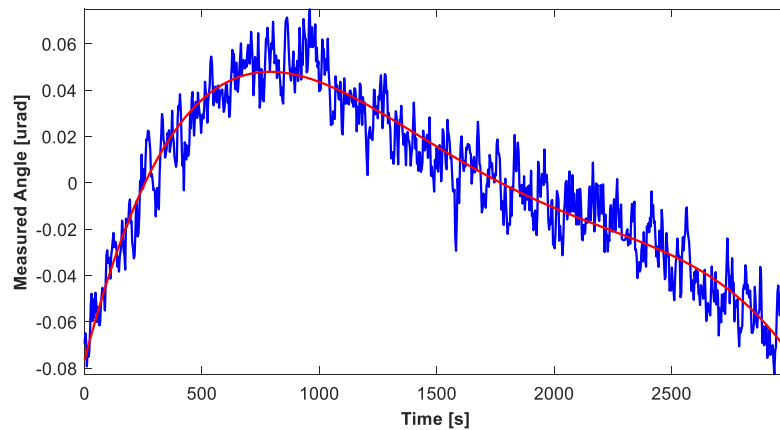


Figure 13. Angular drift of the pitch stage after making an angle change (blue curve). Best fit 4<sup>th</sup> order polynomial (red curve). Such drifts need to be recorded and subtracted from the VeNOM data to improve accuracy.

To assess its dynamic performance, the pitch stage was rotated at a rate of  $5 \mu\text{rad/s}$ , whilst monitoring the actual angle using AC3. Figure 14 shows the linearity errors of the pitch stage, which is the difference between the demand and measured angles. This error needs to be compensated when calculating the motion profile of the X-axis to match to the slope range of the mirror under test.

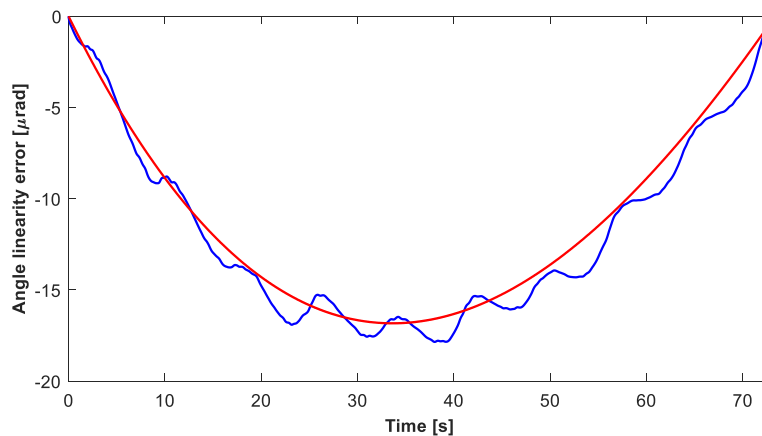


Figure 14. Linearity error of the pitch stage (difference between demand angle and that measured by AC3), shown in the blue curve, versus a best fit 3<sup>rd</sup> order polynomial (red curve). Such errors need to be monitored in real-time and removed from the VeNOM data to improve system accuracy.

In conclusion, the simple, motorized pitch stage has some limitations, both in static and dynamic operational modes, but these issues can easily be corrected using the real-time measurement from AC3. Such corrections confirm the basic suitability of the hardware for dynamic scanning via the new VeNOM concept. A new, in-house goniometer is being built. Once commissioned, closed-loop operation will provide superior stability and resolution of pitch, roll and yaw adjustment of the mirror under test.

#### 4. CONCLUSIONS

We have developed a new instrument: the Diamond-VeNOM which utilises multiple autocollimators, synchronised with motion stage movements, to rapidly measure the optical surface and parasitic motion errors. The optic under test is placed on a motorized tilt stage, and synchronization of motion trajectories and autocollimator data is achieved by temporarily blocking the beam paths of the autocollimators using high-speed electronic shutters, based on triggering signals from positional encoders. Enhanced motion control capabilities enable freeform velocity profiles of the scanning stage, alongside coordinated pitch of the optic under test during each scan. This new concept enables innovative dynamic scanning strategies, including on-the-fly, automated nulling of the optical surface throughout the scan to reduce systematic errors. Preliminary testing of the new system shows that the hardware, software and automation upgrades are capable of delivering the desired performance of dynamic scanning. Overall, using 10X faster, Elcomat5000 autocollimators, and synchronized motion stages, enables 20X faster scanning and innovative dynamic strategies including automated nulling of the optical surface to reduce systematic errors.

#### ACKNOWLEDGEMENTS

This work was carried out with the support of Diamond Light Source. The Authors would like to thank numerous people at Diamond, including: Emilio Perez-Juarez & Adam Howell (Diamond EPICS & Python scripts); Brian Nutter & Nico Rubies (Diamond Motion controls); and Andy Malandain (Diamond Mech. Tech.). We are also indebted to Henry Over & staff at Q-Sys, Netherlands (installation of new controller for NOM), and Ralf Geckeler at PTB and Carsten Schlewitt at Moeller-Wedel for valuable discussions about autocollimators.

#### REFERENCES

1. S. G. Alcock, K. J. S. Sawhney, S. Scott, U. Pedersen, R. Walton, F. Siewert, T. Zeschke, F. Senf, T. Noll, and H. Lammert, "The Diamond-NOM: A non-contact profiler capable of characterizing optical figure error with sub-nanometre repeatability," *Nucl Instrum Methods Phys Res A* **616**, 224–228 (2010).
2. I.-T. Nistea, S. G. Alcock, M. Bazan da Silva, and K. J. S. Sawhney, "The Optical Metrology Laboratory at Diamond: pushing the limits of nano-metrology," *Advances in Metrology for X-Ray and EUV Optics VIII* **1110906**, 5 (2019).
3. S. G. Alcock, I. Nistea, and K. Sawhney, "Nano-metrology: The art of measuring X-ray mirrors with slope errors <100 nrad," *Review of Scientific Instruments* **87**, 1–8 (2016).
4. S. Qian and M. Idir, "Innovative nano-accuracy surface profiler for sub-50 nrad rms mirror test," <https://doi.org/10.1117/12.2247575> **9687**, 81–90 (2016).
5. I. Lacey, J. Adam, G. P. Centers, G. S. Gevorkyan, S. M. Nikitin, B. V. Smith, and V. V. Yashchuk, "Development of a high performance surface slope measuring system for two-dimensional mapping of x-ray optics," <https://doi.org/10.1117/12.2273029> **10385**, 103–115 (2017).
6. R. Geckeler and A. Just, "Distance-dependent influences on angle metrology with autocollimators in deflectometry," <https://doi.org/10.1117/12.793742> **7077**, 85–96 (2008).